Monthly Notices of the ROYAL ASTRONOMICAL SOCIETY **MNRAS Advance Access published September 2, 2013**

MNRAS (2013) doi:10.1093/mnras/stt1460

Probing the Upper Scorpius mass function in the planetary-mass regime⋆

N. Lodieu,[1,2]† P. D. Dobbie,[3] N. J. G. Cross,[4] N. C. Hambly,[4] M. A. Read,[4] R. P. Blake[4] and D. J. E. Floyd[5]

[1]*Instituto de Astrofísica de Canarias (IAC), C/ Vía Láctea s/n, E-38200 La Laguna, Tenerife, Spain*
[2]*Departamento de Astrofísica, Universidad de La Laguna (ULL), E-38206 La Laguna, Tenerife, Spain*
[3]*School of Mathematics & Physics, University of Tasmania, Hobart, TAS 7001, Australia*
[4]*Scottish Universities Physics Alliance (SUPA), Institute for Astronomy, School of Physics and Astronomy, University of Edinburgh, Royal Observatory, Blackford Hill, Edinburgh EH9 3HJ, UK*
[5]*School of Physics, Monash University, Clayton, VIC 3800, Australia*

Accepted 2013 August 2. Received 2013 July 26; in original form 2013 July 3

ABSTRACT

We present the results of a deep *ZYJ* near-infrared survey of 13.5 deg^2 in the Upper Scorpius (USco) OB association. We photometrically selected ∼100 cluster member candidates with masses in the range of 30–5 Jupiters, according to state-of-the-art evolutionary models. We identified 67 *ZYJ* candidates as bona fide members, based on complementary photometry and astrometry. We also extracted five candidates detected with Visible and Infrared Survey Telescope for Astronomy at *YJ* only. One is excluded using deep optical z-band imaging, while two are likely non-members, and three remain as potential members. We conclude that the USco mass function is more likely decreasing in the planetary-mass regime (although a flat mass function cannot yet be discarded), consistent with surveys in other regions.

Key words: techniques: photometric – surveys – brown dwarfs – stars: low-mass – stars: luminosity function, mass function – infrared: stars.

1 INTRODUCTION

The quest for young low-mass objects in the planetary-mass regime aims at addressing two fundamental questions in our understanding of star formation: what is the lowest mass fragment that star formation processes can form? and what is the shape of the initial mass function (IMF; Salpeter 1955; Miller & Scalo 1979; Scalo 1986) below the deuterium-burning limit? Finding planetary-mass objects can help distinguishing among the different star formation models proposed during the past decades. The earliest theoretical prediction by Kumar (1969) suggested a minimum mass of one Jupiter mass ($M_{\rm Jup}$), whereas three-dimensional (3D) opacity-limited hierarchical fragmentation yielded a range between 7 and 10 $M_{\rm Jup}$ (Low & Lynden-Bell 1976; Rees 1976; Silk 1977; Boss 1988). More recent calculations place that limit around (or below) 3–5 $M_{\rm Jup}$ (Boyd & Whitworth 2005; Whitworth & Stamatellos 2006; Forgan & Rice 2011; Rogers & Wadsley 2012).

Several surveys have been carried out over the past years to identify bona fide L and T dwarfs in young star-forming regions to probe the planetary-mass regime and investigate the shape of the substellar mass function. Old field L dwarfs with ages greater than 1 Gyr have typically effective temperatures in the 2200–1400 K range and (model-dependent) masses around 85–50 $M_{\rm Jup}$ (Basri et al. 2000; Leggett et al. 2000; Kirkpatrick 2005), whereas old T dwarfs have temperatures below 1400 K (Burgasser et al. 2006) and masses below ∼50 $M_{\rm Jup}$ (Kirkpatrick 2005). By comparison, 10-Myr-old L and T dwarfs would have masses in the range of ∼20–4 $M_{\rm Jup}$ and ≤4 $M_{\rm Jup}$, respectively (Kirkpatrick 2005). The best-studied region for young L and T dwarfs is σ Orionis, where deep photometric surveys complemented by optical and near-infrared spectroscopy have been conducted (Zapatero Osorio et al. 2000; Barrado y Navascués et al. 2001; Martín et al. 2001; Caballero et al. 2007; Bihain et al. 2009; Peña Ramírez et al. 2011, 2012). The mass function in this region keeps rising in a linear scale ($dN/dM \propto M^{-\alpha}$; Kroupa 2002) from early-type stars (19 solar masses) all the way down to the planetary-mass regime (≤13 $M_{\rm Jup}$) with a possible turnover below 5 $M_{\rm Jup}$ (Peña Ramírez et al. 2012). In NGC 1333, Scholz et al. (2012) estimated that the number of 5–15 $M_{\rm Jup}$ members should be less than 10, implying a decreasing mass function in the planetary-mass regime and a possible cut-off below 6 $M_{\rm Jup}$. Alves de Oliveira et al. (2012) confirmed spectroscopically the first L dwarfs in the ρ Ophiuchus molecular cloud with masses between 10 and 4 $M_{\rm Jup}$, resulting in a mass function in agreement with other regions (Bastian, Covey & Meyer 2010) and the field (Chabrier 2003, 2005). Moreover, Spezzi et al. (2012) reported two potential

⋆Based on observations collected with the ESO VISTA telescope under programme number 089-C.0102(ABC).
† E-mail: nlodieu@iac.es

T-type candidates in the core of the Serpens cloud with masses of a few Jupiter masses if true members. Similarly, Burgess et al. (2009) identified one mid-T-type candidate in IC 348 with a mass between 5 and 1 $M_{\rm Jup}$ but spectroscopy is mandatory to confirm their nature. This T-type candidate is consistent with the extrapolation of the substellar IMF in IC 348 (Alves de Oliveira et al. 2013). A few other L and T dwarf candidates have been announced in older clusters (e.g. Casewell et al. 2007; Bouvier et al. 2008; Hogan et al. 2008; Boudreault & Lodieu 2013) but state-of-the-art models anticipate masses in the midst of the substellar regime (30–50 $M_{\rm Jup}$; Baraffe et al. 1998; Chabrier et al. 2000) because of their older ages (125 Myr for the Pleiades and ∼600 Myr for Praesepe and the Hyades; Perryman et al. 1998; Stauffer, Schultz & Kirkpatrick 1998; Fossati et al. 2008).

Upper Scorpius (hereafter USco) is part of the nearest OB association with the Sun, Scorpius Centaurus. The combination of its distance (145 pc; de Bruijne et al. 1997), young age (5 or 10 Myr depending on the authors; Preibisch & Zinnecker 1999; Pecaut, Mamajek & Bubar 2012; Song, Zuckerman & Bessell 2012) and proper motion (mean value of −25 mas yr^{-1}; de Bruijne et al. 1997; de Zeeuw et al. 1999) makes it an ideal place to look for brown dwarfs and isolated planetary-mass objects to test the theory of the fragmentation limit (Kumar 1969; Low & Lynden-Bell 1976; Rees 1976). The bright end of the USco population has been examined in X-rays (Walter et al. 1994; Preibisch et al. 1998; Kunkel 1999), astrometrically (de Bruijne et al. 1997; de Zeeuw et al. 1999) and spectroscopically (Preibisch & Zinnecker 2002). The low-mass and substellar population has been investigated over the past decade in great details with the advent of modern detectors permitting wide and/or deep surveys (Ardila, Martín & Basri 2000; Martín, Delfosse & Guieu 2004; Lodieu, Hambly & Jameson 2006; Slesnick, Carpenter & Hillenbrand 2006; Lodieu et al. 2007; Slesnick, Hillenbrand & Carpenter 2008; Dawson, Scholz & Ray 2011; Lodieu et al. 2011; Dawson et al. 2013; Lodieu 2013). More recently, we published five potential T-type candidates (Lodieu et al. 2011), discovery not supported by subsequent optical and near-infrared imaging (Lodieu, Ivanov & Dobbie 2013).

In this paper, we present a deep *ZYJ* ($J = 20.5$ mag 100 per cent completeness) and wide (13.5 deg^2) near-infrared survey of the central region of the USco association conducted with the Visible and Infrared Survey Telescope for Astronomy (VISTA; Emerson 2001; Emerson et al. 2004) located in Paranal, Chile. In Section 2, we describe the observations, data reduction and image stacking procedure. In Section 3, we describe complementary data sets from the United Kingdom InfraRed Telescope (UKIRT) Infrared Deep Sky Survey (UKIDSS; Lawrence et al. 2007) Galactic Clusters Survey (GCS) and optical imaging from the 6.5-m Magellan telescope. In Section 4, we detail the photometric selection of member candidates in the USco association. In Section 5, we discuss the shape of the mass function in the planetary-mass regime, comparing the numbers of candidates with our previous determination from the UKIDSS GCS.

2 THE DEEP *ZYJ* SURVEY

2.1 Near-infrared imaging

We performed a near-infrared survey of 13.5 deg^2 in USco (Fig. 1) with the VISTA InfraRed CAMera (VIRCAM; Dalton et al. 2006) mounted on VISTA telescope (Emerson 2001; Emerson et al. 2004) in Paranal, Chile. We choose this part of USco because a subset of this region was imaged as part of the UKIDSS GCS Science verification (Lodieu et al. 2007) and contains many low-mass brown dwarf members confirmed spectroscopically (Lodieu, Dobbie & Hambly 2011). VIRCAM contains 67 million pixels of mean size 0.339 arcsec, offering an instantaneous field of view of 0.6 deg^2. Six 'paw-print' observations are mosaicked together to produce a tile with an area of 1.65 deg^2. We imaged USco in the *ZYJ* filters in service mode between 2012 April and May (see logs of observations in Table 1). In this paper, we use only observing blocks (OBs) completed as part of our ESO (European Southern Observatory) programme 089.C-102(ABC) that complied with our original request (grade A or B according to ESO observing logs): clear sky, grey time with the moon further away than 30° from our target to avoid reflection on the telescope, seeing better than 1.2 arcsec,and air mass less than 1.5 (Table 1).

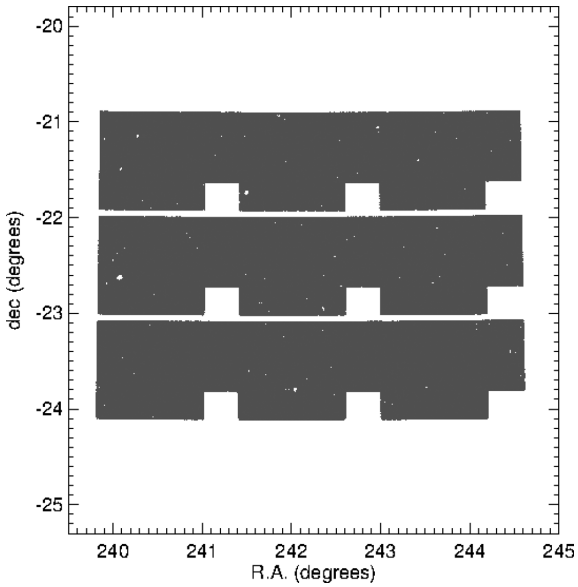

Figure 1. Coverage of the deep VISTA survey in the USco association: 13.5 deg^2 imaged in *ZYJ*.

We employed a similar strategy for all three passbands. We set the detector on-source integrations (DIT) to 50 s, 60 s and 24 s in *Z*, *Y* and *J*, respectively, with six paw-print positions and five jitter positions to create a sky frame (no microstepping). We repeated the DIT twice in the case of *Z* and also repeated the full OBs. The total exposure times amount for 100 min, 30 min and 12 min in *Z*, *Y* and *J*, respectively.

2.2 Data reduction

The data reduction and processing was done as part of the VISTA Data Flow System (VDFS; Emerson et al. 2004), which involves initial quality control at Garching by ESO, OB processing and monthly photometric calibration at Cambridge by the Cambridge Astronomical Survey Unit (CASU)[1] and multi-night processing, matching to external data sets and archiving in Edinburgh by Wide-Field Astronomy Unit (WFAU; Cross et al. 2012).

[1] See http://casu.ast.cam.ac.uk/surveys-projects/vista/technical/ for the latest details.

Table 1. Log of the VISTA/VIRCAM observations. We list the central coordinates of each tile, followed by the dates, averaged seeing, mean ellipticities (Ell) and photometric zero points (ZP) for each tile and each filter.

Tile	RA	Dec.	*Z*				*Y*				*J*			
			Date	Seeing	Ell	ZP	Date	Seeing	Ell	ZP	Date	Seeing	Ell	ZP
	(hh:mm:ss.ss)	(°:′:″)	(yymmdd)	(arcsec)		(mag)	(yymmdd)	(arcsec)		(mag)	(yymmdd)	(arcsec)		(mag)
1_1_1	16:02:05.18	−23:41:04.6	120428	0.974	0.040	23.761	120415	1.302	0.029	23.471	120420	0.955	0.079	23.752
1_1_2	16:08:27.20	−23:41:04.6	120517	0.989	0.052	23.762	120419	1.000	0.042	23.460	120420	0.944	0.048	23.738
1_1_3	16:14:43.50	−23:41:04.6	120516	0.905	0.052	23.754	120417	0.821	0.061	23.466	120428	0.883	0.064	23.753
1_2_1	16:02:05.18	−22:35:33.0	120430	0.885	0.053	23.770	120417	0.960	0.042	23.432	120421	0.703	0.060	23.766
1_2_2	16:08:27.20	−22:35:33.0	120430	0.836	0.064	23.774	120416	0.769	0.058	23.478	120430	0.899	0.048	23.757
1_2_3	16:14:46.40	−22:35:33.0	120516	0.867	0.054	23.754	120419	0.775	0.054	23.463	120428	0.951	0.049	23.738
1_3_1	16:02:05.18	−21:30:01.2	120517	0.935	0.050	23.766	120417	0.777	0.059	23.478	120422	0.778	0.056	23.746
1_3_2	16:08:27.20	−21:30:24.8	120516	1.012	0.044	23.777	120416	0.769	0.055	23.479	120422	0.781	0.061	23.744
1_3_3	16:14:49.66	−21:29:53.3	120516	0.971	0.042	23.768	120418	0.832	0.053	23.473	120422	0.762	0.056	23.736

The initial data reduction of the VISTA images involves the following processes.[2]

(i) Reset correction – similar to bias removal.
(ii) Dark correction – removal of dark current, using exposures taken through a dark filter.
(iii) Linearity correction – take out non-linearities in the detector response.
(iv) Flat-field correction – remove small-scale quantum efficiency variations using twilight flats.
(v) Sky background correction – remove 2D sky background
(vi) Destripe – remove stripe pattern from readout channels. Use detector symmetry.
(vii) Jitter stacking – combine individual, but offset, exposures to remove defects.
(viii) Catalogue generation – extractor finds sources that have more than 4 connected pixels at a threshold of 1.5σ above the sky noise.
(ix) Astrometric and photometric calibration – Uses the Two Micron All Sky Survey (2MASS) all-sky catalogue to obtain an astrometric and photometric calibration. Enhancements, such as zero-point offsets between detectors and the scattered light (illumination) correction, are found later, using a month of data. VISTA data have not been accurately calibrated to the Vega system, as in the case of UKIRT-WFCAM. Instead, it was decided to leave the photometry in the VISTA system and provide colour equations, see Hodgkin et al. (2013, in preparation).
(x) Tile generation – six paw prints are mosaicked together to form a 1.5 deg^2 tile. The catalogue generation is done from a different tile, created after filtering each paw print with a nebulosity filter to remove structure on scales >30 arcsec, to produce smooth backgrounds. Additional steps of grouting to remove effects of mosaicking together paw prints with different point spread functions (PSFs) and reclassification are necessary to produce the best tile catalogues.

All of the individual OBs in the VISTA data are processed in this way. Automated quality control was run to deprecate poor-quality frames. More than 75 per cent of all science frames in this programme passed with over 75 per cent of the deprecated frames coming from OBs which were incomplete or otherwise were set to be re-observed (ESOGRADE C/D/R). At WFAU, OB tiles are grouped into the individual programmes and then processed programme by programme (Cross et al. 2012) matching data across filters and epochs. The main steps are discussed below.

(i) Create tile-paw-print tables linking tile detections to paw-print detections.
(ii) Create deep stacks and tiles. This was necessary for some *Z*-band data which was split over two OBs.
(iii) Band merge deepest data in each band to produce `n089c102Source` table, which is seamed to create a list of unique objects.
(iv) Create neighbour tables between `n089c102Source` and external surveys: UKIDSS DR10 GCS (Lawrence et al. 2007), 2MASS point-source catalogue (Cutri et al. 2003; Skrutskie et al. 2006) and SuperCOSMOS Science Archive (Hambly et al. 2001).
(v) Create best-match and variability tables, so that light curves can be generated for sources. This was done for the *Z* band with the two epochs, with some sources (in overlap regions) having up to eight observations.

2.3 Image stacking and tiling

The creation of deep paw-print stacks and deep tiles from data across many OBs uses the same software (developed by CASU[3]) as was used in the OB stacking and tile creation, except that is bound into the VISTA Science archive software, which selects all the data in the same pointing and filter that passes the quality control, rather than using data with the same OB and group identifiers. The processing of deep stacks and tiles is described in detail in Cross et al. (2012). Deep tiles are not made by stacking OB tiles, but are created by mosaicking six deep paw-print stacks which are in turn created by stacking OB paw-print stacks. This processing sequence gives the best image quality. Photometric calibration of deep paw-print stacks is done by comparing to the component OB stacks; these having been observed in the same filter avoid any colour selection or colour terms that are necessary when comparing with 2MASS. Similarly, deep tiles are calibrated by comparing to the component deep paw prints.

The ($Y - J$, Y) colour–magnitude diagram for all high-quality point sources after the stacking process is shown in Fig. 2. We estimate the depth of our final combined images from the point where the linear fit to the histograms of the numbers of sources as a function of magnitude diverges. We derive 100 per cent completeness

[2] More details at http://apm49.ast.cam.ac.uk/surveys-projects/vista/technical/data-processing

[3] http://apm49.ast.cam.ac.uk/surveys-projects/software-release

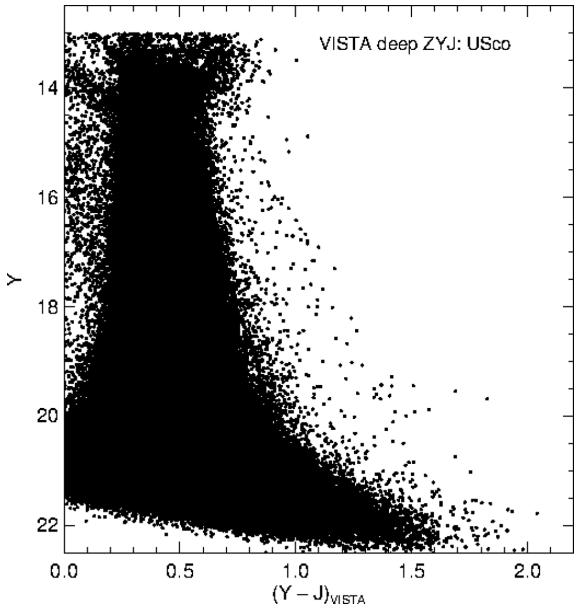

Figure 2. $(Y - J, Y)$ colour–magnitude diagram for all sources detected in the VISTA deep survey.

limits of 22.0 mag, 21.2 mag and 20.5 mag in *Z*, *Y* and *J*, respectively. The saturation limits are 14.0 mag, 14.6 mag and 14.3 mag in *Z*, *Y* and *J*, respectively.

3 COMPLEMENTARY DATA SETS

3.1 The UKIDSS GCS as first epoch

The UKIDSS project, defined in Lawrence et al. (2007), consists of several sub-projects, including the GCS whose main scientific goal is to study the shape and universality of the mass function in the low-mass and substellar regimes. UKIDSS uses the UKIRT Wide Field Camera (WFCAM; Casali et al. 2007). The photometric system is described in Hewett et al. (2006), and the calibration is described in Hodgkin et al. (2009). The pipeline processing and science archive are described in Irwin et al. (2004) and Hambly et al. (2008), respectively. In this section, we use the GCS data to complement our deep *ZYJ* VISTA survey with *H* and *K* photometry and proper motions from the tenth data release (2013 January 14). The 5σ completeness limits of the UKIDSS GCS are typically $Z = 20.2$ mag, $Y = 19.8$ mag, $J = 19.3$ mag, $H = 18.4$ mag and $K = 18.1$ mag (e.g. fig. 2 of Lodieu, Deacon & Hambly 2012; Dye et al. 2006), implying that our VISTA survey is 1.2–1.8 mag deeper than the GCS depending on the filter. The proper motions computed as part of the latest GCS data release take into account the different epochs of observations in all the filters (Collins & Hambly 2012), providing proper motions accurate to 5–10 mas yr^{-1}.

3.2 Magellan/IMACS *z*-band imaging

A number of regions of Upper Sco were observed in the *z* band during 2009 May with the Inamori Magellan Areal Camera and Spectrograph (IMACS) and the 6.5-m Magellan Baade telescope. Total integration times of 90 min were built up through a number of 300-s sub-exposures. IMACS is a wide-field imaging system (or multi-object spectrograph) in which light from the Gregorian secondary of the telescope is fed to one of two cameras: short (f/2.5) or long (f/4.3). The short camera, used for these observations, is constructed around a mosaic of eight 2048 × 4096 pixel *E2V* CCDs and covers a 27.5 × 27.5 arcmin^2 (0.20 arcsec pixel) area of sky per pointing. However, it suffers from strong vignetting at distances more that 15 arcmin from the field centre.

The data frames were reduced using the CASU CCD reduction toolkit (Irwin & Lewis 2001) to follow standard steps, namely subtraction of the bias, flat-fielding, astrometric calibration and co-addition. We performed aperture photometry on the reduced images using a circular window with a diameter of 1.5 × the full width half-maximum of the mean PSF (∼0.6–0.7 arcsec). Finally, we cross-correlated our optical photometry with our catalogue of near-infrared data and transformed our instrumental magnitudes on to approximately the VISTA *Z*-band natural system.

4 PHOTOMETRIC SELECTION OF MEMBER CANDIDATES IN USco

4.1 Contents of the VISTA catalogue

We wrote a Structure Query Language (SQL) sent to the VISTA Science archive (Cross et al. 2012) to retrieve all good-quality point sources present in the VISTA *ZYJ* catalogue. We imposed quality criteria set by the `ppErrBits` parameters (less than 256) as well as point-source criteria determined by the `Class` and `ClassStat` parameters. We considered only sources fainter than *Z*, $Y = 13$ mag and $J = 12$ mag although saturation limits are fainter by at least 1 mag. We also allowed for *Z*-band non-detection to improve our completeness at the faint end.

Our deep VISTA survey overlaps with the *HK* coverage from the GCS DR10. Our SQL query includes a cross-match of both catalogues using a matching radius of 3 arcsec. Hence, each source in the VISTA catalogue has a counterpart in the GCS database, if there is one found within the matching radius. The final catalogue provides *ZYJHK*1*K*2 photometry (two epochs in *K*) for 1098 027 point sources,[4] along with their proper motions and associated errors from the GCS DR10.

These proper motions and their associated errors are measured from the multiple epochs available from the GCS, calculating a mean epoch and a making linear least-squares fit on the errors of the positions with standard error propagation. A factor for the noise floor has been added to correct for the fact that the centroid errors are not getting better with brighter magnitudes but instead reach a plateau. The procedure is detailed at length in Collins & Hambly (2012).

4.2 Deep *ZYJ* survey

We applied photometric cuts in two colour–magnitude diagrams to select member candidates in the 13.5 deg^2 surveyed in USco, based on the location of known USco members located in the VISTA coverage (open squares in Fig. 3), which are confirmed photometrically, astrometrically and spectroscopically (Lodieu et al. 2011; Lodieu 2013). We recovered 37 known members from our previous work, including 12 fainter than $Y = 14.6$ mag (open squares in Figs 3 and 4; Lodieu et al. 2011).

We restrain our photometric selection to sources fainter than $Y = 14.6$ mag (unsaturated objects) and brighter than the 100 per cent completeness limits of our survey in *Y* and *J* only.

[4] We plan to make this catalogue available to the community via Vizier at the Centre de Données de Strasbourg.

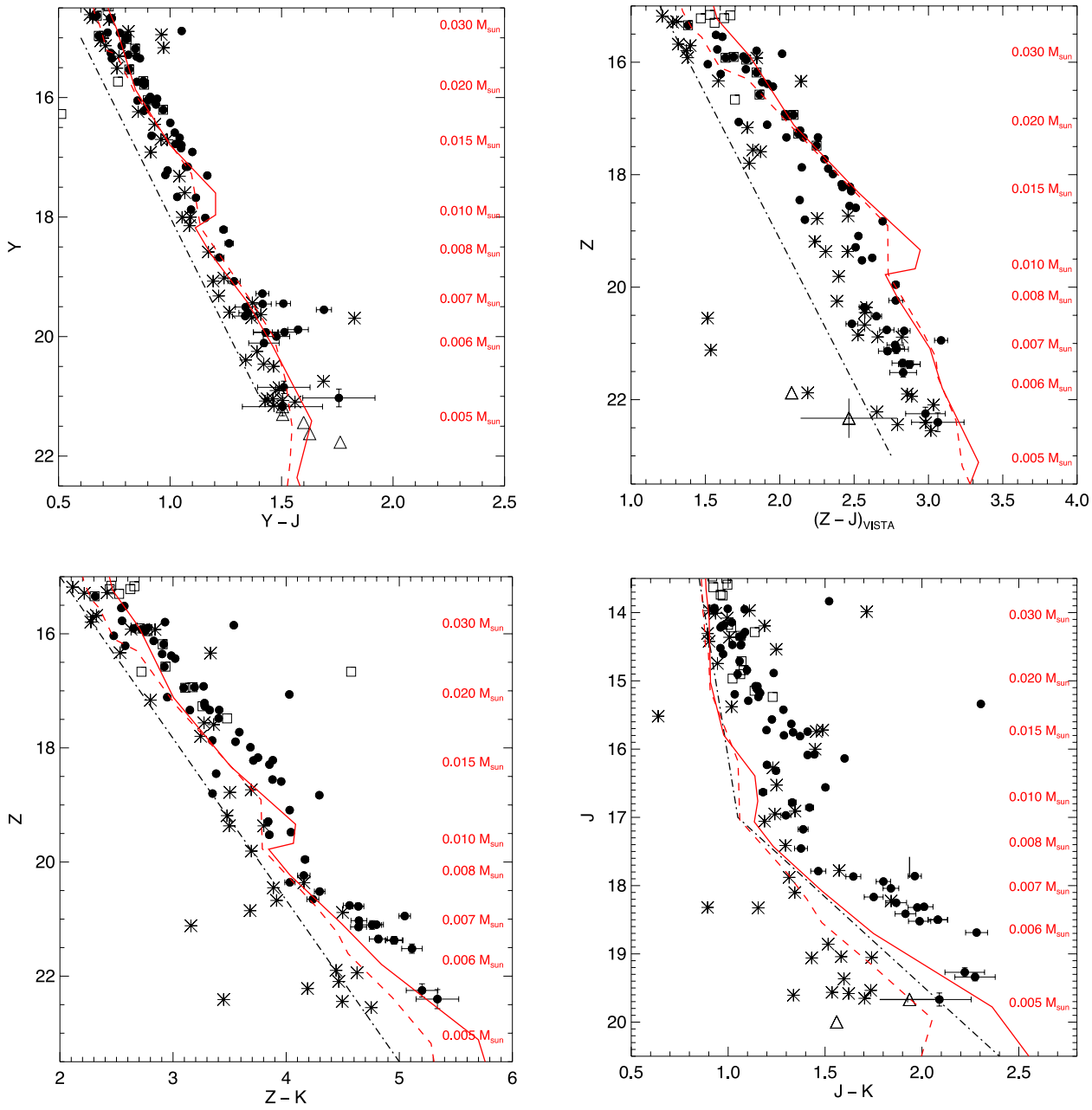

Figure 3. $(Y - J, Y)$, $(Z - J, Z)$, $(Z - K, Z)$ and $(J - K, J)$ colour–magnitude diagrams (ordered following the photometric selection described in this work) for member candidates identified photometrically in the VISTA (filled dots). Open squares are previously confirmed USco spectroscopic members (Lodieu et al. 2011). Photometric non-members are marked with an asterisk. *YJ*-only candidates with *Z*-band dropouts are plotted as open triangles. Uncertainties in magnitudes and colours are included only for member candidates: some error bars are not visible because they are smaller than the size of the dots. Overplotted are the 5 and 10 Myr BT-Settl isochrones (red lines) shifted at the distance of USco (Allard, Homeier & Freytag 2012). The associated masses are quoted on the right-hand side, assuming an age of 5 Myr and a distance of 145 pc for USco.

We started our photometric selection in the $(Y - J, Y)$ colour–magnitude diagram (Fig. 3) because it offers the greatest sensitivity to substellar members. We kept only sources to the right of the lines (dot–dashed lines in Fig. 3) defined by

(i) $(Y - J, Y) = (0.6,15.0)$ to $(1.4,21.0)$;
(ii) $(Z - J, Z) = (1.0,14.0)$ to $(2.75,23.0)$.

The *YJ* selection returned 109 candidates, number reduced to 101 when applying the photometric cuts in the $(Z - J, Z)$ diagram. In Fig. 3, we overplotted the BT-Settl models (Allard et al. 2012) for the UKIDSS filter set (Hewett et al. 2006) although our survey uses the VISTA *ZYJ* filters. However, these three VISTA filters are identical to the filters installed on UKIRT/WFCAM at the 1 per cent level.[5]

4.3 Improving the photometric selection

In this section we improve on our three-band photometric selection using proper motions and near-infrared *HK* photometry and proper

[5] http://apm49.ast.cam.ac.uk/surveys-projects/vista/technical/filter-set

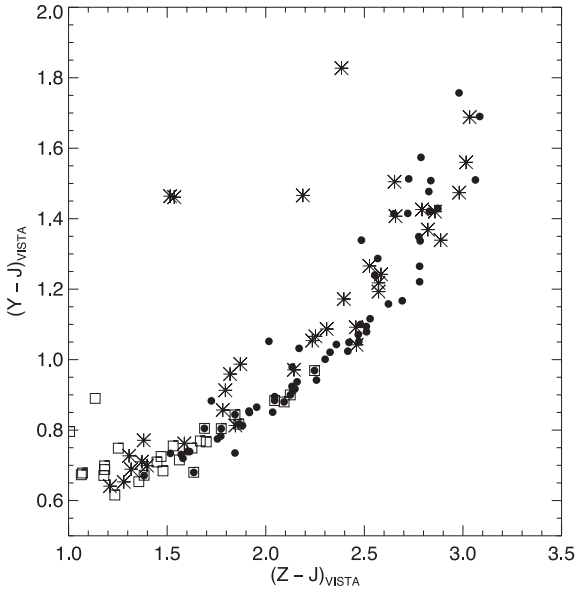

Figure 4. ($Z - J$, $Y - J$) colour–colour diagram for USco member candidates identified in the VISTA survey. Symbols are the same as in Fig. 3.

motions from the UKIDSS GCS DR10 to confirm (or otherwise) photometric candidates identified in the previous section.

We selected point sources brighter than $J = 18.5$ mag whose errors on the proper motions are within 4σ of the mean USco proper motion (i.e. more than 99.99 per cent completeness), centred at $(-6, -20)$ mas yr^{-1}. Fainter sources were kept because they will be fainter in UKIDSS than VISTA, yielding large errors on the source centroid. This selection yielded 66+17 = 83 candidates.

Secondly, we took advantage of the additional *H*- and *K*-band imaging from the UKIDSS GCS DR10 to improve on our photometric and astrometric selections. The ($Z - K$, Z) and ($J - K$, J) diagrams involving Z and J photometry from VISTA and K photometry from GCS DR10 are displayed in Fig. 3. We applied the following photometric cuts (dot–dashed lines in Fig. 3):

(i) $(Z - K, Z) = (2.0,15.0)$ to $(5.0,23.5)$;
(ii) $(J - K, J) = (0.85,13.5)$ to $(1.05,17.0)$;
(iii) $(J - K, J) = (1.05,13.5)$ to $(2.9,20.5)$.

This selection returned 67 candidates (Table 2), which represent our final sample of bona fide USco members in 13.5 deg^2 down to a depth of $J = 20.5$ mag, corresponding to $\sim 5\,M_{\rm Jup}$ according to the BT-Settl models at 5 Myr (Allard et al. 2012). We plot these new members as filled dots in the colour–magnitude and colour–colour diagrams displayed in Figs 3 and 4. The candidates classified as photometric and/or astrometric non-members are plotted as asterisks in Figs 3 and 4, and are listed in Table 3.

We point out that the BT-Settl models at 5 Myr (or 10 Myr) have trouble reproducing the observed USco sequence in the ($Z - J$, Z) colour–magnitude diagram below the deuterium-burning limit. Moreover, the predicted $J - K$ colours are too blue, as seen in the ($J - K$, J) diagram (Fig. 3). However, the kink predicted by the models at the deuterium-burning limit is clearly observed in the USco sequence, demonstrating that we are clearly reaching sources with masses in the planetary-mass regime, independently of the inherent uncertainties in the assignment of masses at young ages (Baraffe et al. 2002; Hillenbrand & White 2004).

4.4 *Z*-band dropouts

We searched for *Z*-band dropouts, selecting all sources lying to the right of a line running from $(Y - J, Y) = (1.0, 20.0)$ to $(1.75, 22.0)$ in that diagram. This query returned 30 candidates. After inspecting the VISTA images, we rejected 25 of them because we can see a detection in the *Z*-band images at the position of the object in spite of the magnitude in this passband not being catalogued. The remaining five candidates are listed in Table 4.

We found *K*-band magnitudes from the GCS DR10 for two of five *YJ* candidates with *Z* dropouts (Table 4). One of them (16:11:48.92−21:05:28.6) has two *K*-band measurements (Table 4), indicating a possible intrinsic variability. Its $J - K$ colour spans the 1.78–2.09 mag range, placing it close to the 10-Myr isochrone in the ($J - K$, J) diagram but to the blue of the cluster sequence. The other source with a *K*-band detection would be bluer, with $J - K = 1.56$ mag, suggesting that it not a member unless the sequence turns to the blue if we reach the L/T transition (models predict effective temperatures in the 1400–1200 K range for a $5\,M_{\rm Jup}$ object at 5–10 Myr). The other three candidates are undetected in the *K* band, implying $J - K$ colours bluer than 1.6–1.8 mag assuming a 5σ completeness limit of 18.2 mag for the GCS *K*-band depth.

Table 2. Sample of 67 USco member candidates in the VISTA deep survey: we list their coordinates, photometry, proper motions in both directions (in mas yr^{-1}) and their associated error bars. The complete table is available in the electronic version, only a subset is shown here for its content.

RA	Dec.	$Z \pm$ err	$Y \pm$ err	$J \pm$ err	$H \pm$ err	$K1 \pm$ err	$K2 \pm$ err	$\mu_\alpha \cos\delta \pm$ err	$\mu_\delta \pm$ err
15:59:36.38	−22:14:15.9	19.523 ± 0.014	18.210 ± 0.013	16.970 ± 0.009	16.341 ± 0.028	15.672 ± 0.024	15.638 ± 0.015	−0.05 ± 8.58	−19.40 ± 8.58
15:59:48.01	−22:27:16.5	15.899 ± 0.002	14.919 ± 0.002	14.144 ± 0.001	13.610 ± 0.003	13.125 ± 0.003	13.147 ± 0.002	−1.48 ± 6.83	−14.09 ± 6.83
–	–	–	–	–	–	–	–	–	–
16:17:00.53	−22:12:53.9	18.170 ± 0.007	16.778 ± 0.004	15.754 ± 0.004	15.084 ± 0.008	14.419 ± 0.007	14.468 ± 0.005	2.37 ± 6.99	−24.16 ± 6.99
16:17:02.61	−20:54:49.4	15.548 ± 0.002	14.673 ± 0.001	13.934 ± 0.001	13.440 ± 0.003	13.005 ± 0.003	13.002 ± 0.002	−3.39 ± 4.44	−18.62 ± 4.44

Table 3. Sample of 43 USco candidates classified as photometric and/or astrometric non-members. This table provides their coordinates, photometry, proper motions with their uncertainties. The complete table is available in the electronic version, only a subset is shown here for its content.

RA	Dec.	$Z \pm$ err	$Y \pm$ err	$J \pm$ err	$H \pm$ err	$K1 \pm$ err	$K2 \pm$ err	$\mu_\alpha \cos\delta \pm$ err	$\mu_\delta \pm$ err
15:59:37.56	−22:54:16.3	16.338 ± 0.003	15.166 ± 0.002	14.195 ± 0.001	13.554 ± 0.003	13.007 ± 0.002	13.011 ± 0.002	−225.61 ± 6.82	−214.84 ± 6.82
15:59:57.99	−21:54:22.4	22.410 ± 0.159	20.903 ± 0.109	19.429 ± 0.074	19.427 ± 0.331	18.963 ± 0.385	17.848 ± 0.126	−40.79 ± 9.66	−29.17 ± 9.66
–	–	–	–	–	–	–	–	–	–
16:18:25.46	−23:40:53.5	17.797 ± 0.007	16.915 ± 0.005	16.002 ± 0.004	15.051 ± 0.007	14.553 ± 0.008	14.525 ± 0.006	−11.99 ± 2.27	19.74 ± 2.27
16:18:25.65	−23:42:45.4	15.278 ± 0.002	14.698 ± 0.001	13.971 ± 0.001	13.223 ± 0.002	12.861 ± 0.002	12.867 ± 0.002	−3.73 ± 2.19	−1.63 ± 2.19

Table 4. *Z*-band dropouts (or *YJ*-only) candidates in USco. The *K*-band photometry is from the UKIDSS GCS DR10.

RA hh:mm:ss.ss	Dec. (°:′:″)	$Y \pm$ err (mag)	$J \pm$ err (mag)	$K \pm$ err (mag)
16:11:48.92	−21:05:28.6	21.173 ± 0.152	19.669 ± 0.096	17.887 ± 0.108[a]
16:13:06.55	−22:55:32.7	21.303 ± 0.155	19.798 ± 0.090	>18.2[b]
16:12:51.83	−23:16:50.0	21.437 ± 0.203	19.838 ± 0.095	>18.2[c]
16:16:21.04	−23:55:20.1	21.624 ± 0.241	19.998 ± 0.109	18.438 ± 0.167
16:10:27.63	−23:05:54.3	21.767 ± 0.438	20.004 ± 0.145	>18.2

Note: [a]We list the *K*-band magnitude with the lowest error bar: the other measurement available from GCS DR10 gives $K = 17.579 \pm 0.133$ mag.
[b]This object, covered by our IMACS survey, has a magnitude of 21.878 ($Z - J = 20.8$ mag) and is rejected as a member.
[c]This candidate lies in the vignetted part of the IMACS detector. We estimated its $Z - J$ colour to 2.14–2.79 mag.

We note that all five *YJ* candidates lie outside the Gran Telescopio de Canarias Optical System for Imaging and low-intermediate Resolution Integrated Spectrograph coverage discussed in Lodieu et al. (2013). However, we detected two of these five sources in deep Magellan/IMACS data. One candidate (16:13:06.55−22:55:32.7) is clearly detected on the IMACS images at 0.145 arcsec from the VISTA detection. We derived a magnitude of 21.878, implying a $Z - J$ colour of 2.08 mag (Table 4), placing this object clearly to the blue part of the cluster sequence. Hence, we discard this object as a member of USco. The second candidate (16:12:51.83−23:16:50.0) lies in the region of the detector which suffered strong vignetting, yielding large error bar on the photometry. We estimate its magnitude to 21.98–22.68, implying a $Z - J$ colour in the 2.14–2.79 mag (Table 4). This object also lies to the blue of the cluster sequence but we cannot fully discard it until we obtain a better estimate of its magnitude. At this stage, we are unable to discard the other candidates because they could be L/T transition members in USco: deeper optical imaging and near-infrared spectroscopy can confirm this argument as well as their nature.

5 DISCUSSION ON THE MASS FUNCTION

Before looking at the shape of the USco mass function in the planetary-mass regime, we discuss the mass estimates and place our work into context.

Masses at young ages (<10 Myr) are difficult to measure and can be very uncertain (Baraffe et al. 2002) and depend also on the models considered during the analysis (Hillenbrand & White 2004). The lack of spectroscopy for the lowest and youngest brown dwarf candidates identified photometrically to date in star-forming regions and clusters hampers our ability to estimate masses accurately. To estimate the depth of our VISTA survey, we rely on the latest BT-Settl models (Allard et al. 2012), assuming a distance of 145 pc and ages of 5 and 10 Myr for USco. According to these models, a $5\,M_{\rm Jup}$ brown dwarf with an effective temperature of 1400–1200 K in USco has apparent magnitudes of $Z \sim 23.1$–23.9 mag, $Y \sim 21.4$–22.1 mag and $J \sim 19.8$–20.6 mag, respectively (depending on the age chosen). These *J*-band values are consistent with our 100 per cent completeness limit so we are sensitive to $5\,M_{\rm Jup}$ brown dwarfs in USco. However, the *Y*- and *Z*-band magnitudes of a $5\,M_{\rm Jup}$ brown dwarf in USco are fainter than our completeness limits, implying that we are complete down to $6\,M_{\rm Jup}$ ($Y = 20.16$ mag and $Z = 21.79$ mag).

In terms of magnitude, our survey is shallower than the deep $ZYJHK_{\rm s}$ VISTA survey in σ Orionis ($J = 21$ mag versus 20.5 mag) by Peña Ramírez et al. (2012). However, both surveys have very similar depths in terms of mass because σ Ori is further away than USco (352 pc versus 145 pc), resulting in a $5\,M_{\rm Jup}$ having $J = 20.53$ mag in σ Ori and $J = 20.57$ Myr for USco, assuming 10 Myr ($J = 19.77$ mag at 5 Myr in USco). The coolest spectroscopically confirmed member of σ Ori, sOri 65 ($Y = 21.1 \pm 0.1$; $J = 20.3 \pm 0.1$ mag; L3.5; Zapatero Osorio et al. 2000; Sherry, Walter & Wolk 2004; Scholz & Jayawardhana 2008; Peña Ramírez et al. 2012) is close to our 100 per cent completeness so we predict that our VISTA survey is sensitive to mid-L dwarfs in USco, considering the similarities between both surveys. Nonetheless, we cannot discard that we are sensitive to L/T transition objects because of the similar apparent magnitudes observed for field brown dwarfs across the mid-L to mid-T regime (e.g. Leggett et al. 2010).

To address the shape of the USco mass function in the planetary-mass regime (Salpeter 1955; Miller & Scalo 1979; Scalo 1986), we divided our sample into two mass bins of equal size in a logarithmic scale. We counted the number of candidates in the 20–10 and 10–$5\,M_{\rm Jup}$ bins, resulting in a ratio of 24/22 = 1.09 (27/16 = 1.69), respectively, using the *J*-band filter and assuming an age of 5 Myr for USco (values in brackets are for 10 Myr). If we consider the *Y*-band filter instead, the ratios become 25/21 = 1.19 (5 Myr) and 30/16 = 1.88 (10 Myr), respectively. These ratios are upper limits because our survey is complete down to $6\,M_{\rm Jup}$ and incomplete in the 6–$5\,M_{\rm Jup}$ interval. Therefore, we conclude that the USco mass function is more likely to decrease in the planetary-mass regime although a flat mass function cannot be discarded for an age of 5 Myr until proper motions or near-infrared spectroscopy is obtained for all candidates. Our conclusions agree with the possible turnover of the mass function in the planetary-mass regime observed in σ Ori (Peña Ramírez et al. 2012) and NGC 1333 (Scholz et al. 2012) but at odds with the rising mass function seen in ρ Oph (Marsh et al. 2010; Barsony et al. 2012).

Our future goal would be to reach $1\,M_{\rm Jup}$ to test the various theoretical models proposing discrepant minimum masses: self-gravitating disc fragmentation or gravitationally unstable discs lead to minimum masses of 3–$5\,M_{\rm Jup}$, whereas fragmentation of a shock-compressed layer suggests minimum masses below $3\,M_{\rm Jup}$, in agreement with the original prediction by Kumar (1969). The latest evolutionary BT-Settl models predict absolute *J* magnitudes 1.5–2 mag fainter for a $3\,M_{\rm Jup}$ compared to a $5\,M_{\rm Jup}$ brown dwarfs at 5 or 10 Myr, consistent with differences predicted by the COND models (Baraffe et al. 2002). Similarly, the COND models predict that a $1\,M_{\rm Jup}$ object in USco would be 3 mag fainter than a $3\,M_{\rm Jup}$ in *J*, implying that we would need a survey down to $J \sim 25$ mag, depth very difficult to achieve from the ground over a wide area (at least six square degrees are needed for statistical purposes).[6] Although not ideal for large-scale surveys, near- and mid-infrared capabilities of the *James Webb Space Telescope* seem to be the only option to address the issue of the fragmentation limit by the end of the decade.

ACKNOWLEDGEMENTS

NL was funded by the Ramón y Cajal fellowship number 08-303-01-02 and the national programme AYA2010-19136 funded by the Spanish ministry of Science and Innovation.

This work is based on observations made with the ESO VISTA telescope at the Paranal Observatory under programme ID 089.

[6] The five-year UltraVISTA public survey aims at reaching 5σ depths of $Y \sim 26$ mag, $J \sim 25.5$ mag in the Vega system over 1.5 deg^2 (McCracken et al. 2012).

C-0102(ABC) in service mode and in visitor mode with the 6.5-m Magellan telescope at Las Campanas Observatory Carnegie Institution of Washington.

This work is based in part on data obtained as part of the UKIRT Infrared Deep Sky Survey (UKIDSS). We thank our colleagues at the UK Astronomy Technology Centre, the Joint Astronomy Centre in Hawaii, the Cambridge Astronomical Survey and Edinburgh Wide Field Astronomy Units for building and operating WFCAM and its associated data flow system.

This research has made use of the Simbad and Vizier (Ochsenbein, Bauer & Marcout 2000) data bases, operated at the Centre de Données Astronomiques de Strasbourg (CDS), and of NASA's Astrophysics Data System Bibliographic Services (ADS).

REFERENCES

Allard F., Homeier D., Freytag B., 2012, Phil. Trans. R. Soc. A, 370, 2765
Alves de Oliveira C., Moraux E., Bouvier J., Bouy H., 2012, A&A, 539, A151
Alves de Oliveira C., Moraux E., Bouvier J., Duchêne G., Bouy H., Maschberger T., Hudelot P., 2013, A&A, 549, A123
Ardila D., Martín E., Basri G., 2000, AJ, 120, 479
Baraffe I., Chabrier G., Allard F., Hauschildt P. H., 1998, A&A, 337, 403
Baraffe I., Chabrier G., Allard F., Hauschildt P. H., 2002, A&A, 382, 563
Barrado y Navascués D., Zapatero Osorio M. R., Béjar V. J. S., Rebolo R., Martín E. L., Mundt R., Bailer-Jones C. A. L., 2001, A&A, 377, L9
Barsony M., Haisch K. E., Marsh K. A., McCarthy C., 2012, ApJ, 751, 22
Basri G., Mohanty S., Allard F., Hauschildt P. H., Delfosse X., Martín E. L., Forveille T., Goldman B., 2000, ApJ, 538, 363
Bastian N., Covey K. R., Meyer M. R., 2010, ARA&A, 48, 339
Bihain G. et al., 2009, A&A, 506, 1169
Boss A. P., 1988, ApJ, 331, 370
Boudreault S., Lodieu N., 2013, MNRAS, 434, 142
Bouvier J. et al., 2008, A&A, 481, 661
Boyd D. F. A., Whitworth A. P., 2005, A&A, 430, 1059
Burgasser A. J., Geballe T. R., Leggett S. K., Kirkpatrick J. D., Golimowski D. A., 2006, ApJ, 637, 1067
Burgess A. S. M., Moraux E., Bouvier J., Marmo C., Albert L., Bouy H., 2009, A&A, 508, 823
Caballero J. A. et al., 2007, A&A, 470, 903
Casali M. et al., 2007, A&A, 467, 777
Casewell S. L., Dobbie P. D., Hodgkin S. T., Moraux E., Jameson R. F., Hambly N. C., Irwin J., Lodieu N., 2007, MNRAS, 378, 1131
Chabrier G., 2003, PASP, 115, 763
Chabrier G., 2005, in Corbelli E., Palla F., Zinnecker H., eds, Astrophysics and Space Science Library, Vol. 327, The Initial Mass Function 50 Years Later. Springer, Berlin, p. 41
Chabrier G., Baraffe I., Allard F., Hauschildt P., 2000, ApJ, 542, 464
Collins R., Hambly N., 2012, in Ballester P., Egret D., Lorente N. P. F., eds, ASP Conf. Ser. Vol. 461, Astronomical Data Analysis Software and Systems XXI. Astron. Soc. Pac., San Francisco, p. 525
Cross N. J. G. et al., 2012, A&A, 548, A119
Cutri R. M. et al., 2003, 2MASS All Sky Catalog of point sources, p. 2246
Dalton G. B. et al., 2006, Proc. SPIE, 6269, 62690X
Dawson P., Scholz A., Ray T. P., 2011, MNRAS, 418, 1231
Dawson P., Scholz A., Ray T. P., Marsh K. A., Wood K., Natta A., Padgett D., Ressler M. E., 2013, MNRAS, 429, 903
de Bruijne J. H. J., Hoogerwerf R., Brown A. G. A., Aguilar L. A., de Zeeuw P. T., 1997, in ESA SP-402: *Hipparcos* – Venice '97 Improved Methods for Identifying Moving Groups. p. 575
de Zeeuw P. T., Hoogerwerf R., de Bruijne J. H. J., Brown A. G. A., Blaauw A., 1999, AJ, 117, 354
Dye S. et al., 2006, MNRAS, 372, 1227
Emerson J. P., 2001, in Clowes R., Adamson A., Bromage G., eds, ASP Conf. Ser. Vol. 232, The New Era of Wide Field Astronomy. Astron. Soc. Pac., San Francisco, p. 339
Emerson J. P., Sutherland W. J., McPherson A. M., Craig S. C., Dalton G. B., Ward A. K., 2004, The Messenger, 117, 27
Forgan D., Rice K., 2011, MNRAS, 417, 1928
Fossati L., Bagnulo S., Landstreet J., Wade G., Kochukhov O., Monier R., Weiss W., Gebran M., 2008, A&A, 483, 891
Hambly N. C. et al., 2001, MNRAS, 326, 1279
Hambly N. C. et al., 2008, MNRAS, 384, 637
Hewett P. C., Warren S. J., Leggett S. K., Hodgkin S. T., 2006, MNRAS, 367, 454
Hillenbrand L. A., White R. J., 2004, ApJ, 604, 741
Hodgkin S. T., Irwin M. J., Hewett P. C., Warren S. J., 2009, MNRAS, 394, 675
Hogan E., Jameson R. F., Casewell S. L., Osbourne S. L., Hambly N. C., 2008, MNRAS, 388, 495
Irwin M., Lewis J., 2001, New Astron. Rev., 45, 105
Irwin M. J. et al., 2004, in Quinn P. J., Bridger A., eds, Proc. SPIE. Vol. 5493, Optimizing Scientific Return for Astronomy through Information Technologies. SPIE, Bellingham, p. 411
Kirkpatrick J. D., 2005, ARA&A, 43, 195
Kroupa P., 2002, Sci, 295, 82
Kumar S. S., 1969, in Kumar S. S., ed., Low-Luminosity Stars, Proceedings of the Symposium held at University of Virginia, 1968. Gordon and Breach, Sci. Publ., New York, p. 255
Kunkel M., 1999, PhD Thesis, Julius-Maximilians-Universität
Lawrence A. et al., 2007, MNRAS, 379, 1599
Leggett S. K. et al., 2000, ApJ, 536, L35
Leggett S. K. et al., 2010, ApJ, 710, 1627
Lodieu N., 2013, MNRAS, 431, 3222
Lodieu N., Deacon N. R., Hambly N. C., 2012, MNRAS, 422, 1495
Lodieu N., Dobbie P. D., Hambly N. C., 2011, A&A, 527, A24
Lodieu N., Hambly N. C., Dobbie P. D., Cross N. J. G., Christensen L., Martin E. L., Valdivielso L., 2011, MNRAS, 418, 2604
Lodieu N., Hambly N. C., Jameson R. F., 2006, MNRAS, 373, 95
Lodieu N., Hambly N. C., Jameson R. F., Hodgkin S. T., Carraro G., Kendall T. R., 2007, MNRAS, 374, 372
Lodieu N., Ivanov V. D., Dobbie P. D., 2013, MNRAS, 430, 1784
Low C., Lynden-Bell D., 1976, MNRAS, 176, 367
Marsh K. A., Plavchan P., Kirkpatrick J. D., Lowrance P. J., Cutri R. M., Velusamy T., 2010, ApJ, 719, 550
Martín E. L., Delfosse X., Guieu S., 2004, AJ, 127, 449
Martín E. L., Zapatero Osorio M. R., Barrado y Navascués D., Béjar V. J. S., Rebolo R., 2001, ApJ, 558, L117
McCracken H. J. et al., 2012, A&A, 544, A156
Miller G. E., Scalo J. M., 1979, ApJS, 41, 513
Ochsenbein F., Bauer P., Marcout J., 2000, A&AS, 143, 23
Pecaut M. J., Mamajek E. E., Bubar E. J., 2012, ApJ, 746, 154
Peña Ramírez K., Béjar V. J. S., Zapatero Osorio M. R., Petr-Gotzens M. G., Martín E. L., 2012, ApJ, 754, 30
Peña Ramírez K., Zapatero Osorio M. R., Béjar V. J. S., Rebolo R., Bihain G., 2011, A&A, 532, A42
Perryman M. A. C. et al., 1998, A&A, 331, 81
Preibisch T., Guenther E., Zinnecker H., Sterzik M., Frink S., Roeser S., 1998, A&A, 333, 619
Preibisch T., Zinnecker H., 1999, AJ, 117, 2381
Preibisch T., Zinnecker H., 2002, AJ, 123, 1613
Rees M. J., 1976, MNRAS, 176, 483
Rogers P. D., Wadsley J., 2012, MNRAS, 423, 1896
Salpeter E. E., 1955, ApJ, 121, 161
Scalo J. M., 1986, Fundam. Cosm. Phys., 11, 1
Scholz A., Jayawardhana R., 2008, ApJ, 672, L49
Scholz A., Jayawardhana R., Muzic K., Geers V., Tamura M., Tanaka I., 2012, ApJ, 756, 24
Sherry W. H., Walter F. M., Wolk S. J., 2004, AJ, 128, 2316
Silk J., 1977, ApJ, 214, 152
Skrutskie M. F. et al., 2006, AJ, 131, 1163

Slesnick C. L., Carpenter J. M., Hillenbrand L. A., 2006, AJ, 131, 3016
Slesnick C. L., Hillenbrand L. A., Carpenter J. M., 2008, ApJ, 688, 377
Song I., Zuckerman B., Bessell M. S., 2012, AJ, 144, 8
Spezzi L., Alves de Oliveira C., Moraux E., Bouvier J., Winston E., Hudelot P., Bouy H., Cuillandre J.-C., 2012, A&A, 545, A105
Stauffer J. R., Schultz G., Kirkpatrick J. D., 1998, ApJ, 499, 219
Walter F. M., Vrba F. J., Mathieu R. D., Brown A., Myers P. C., 1994, AJ, 107, 692
Whitworth A. P., Stamatellos D., 2006, A&A, 458, 817
Zapatero Osorio M. R., Béjar V. J. S., Martín E. L., Rebolo R., Barrado y Navascués D., Bailer-Jones C. A. L., Mundt R., 2000, Sci, 290, 103

SUPPORTING INFORMATION

Additional Supporting Information may be found in the online version of this article:

Table 2. 67 USco member candidates in the VISTA deep survey: we list their coordinates, photometry, proper motions in both directions (in mas yr^{-1}) and their associated error bars.

Table 3. 43 USco candidates classified as photometric and/or astrometric non-members. This table provides their coordinates, photometry and proper motions with their uncertainties (http://mnras.oxfordjournals.org/lookup/suppl/doi:10.1093/mnras/stt1460/-/DC1).

Please note: Oxford University Press are not responsible for the content or functionality of any supporting materials supplied by the authors. Any queries (other than missing material) should be directed to the corresponding author for the article.

This paper has been typeset from a TEX/LATEX file prepared by the author.